이학석사 학위논문

I. Studies on the shape-dependent catalytic activities of Pd nanoparticles

II. Studies on the transition metals immobilized on multi-wall carbon nanotubes

I. 팔라듐 나노입자의 모양에 따른 촉매 활성에 관한 연구

II. 탄소 나노튜브의 작용기와 전이금속 도입에 관한 연구

2012년 8월

서울대학교 대학원
화학부 유기화학 전공
정 한 샘

CONTENTS

Abstract

Part I. Studies on the shape-dependent catalytic activities of Pd nanoparticles

Part I describes the study on the selective hydrogenation of alkynes into alkenes over palladium nanocatalysts having different shapes. Palladium nanocubes were simply prepared in an aqueous solution by reducing Na_2PdCl_4 with L-ascorbic acid in the presence of bromide ions as a capping agent to promote the formation of [100] facets. To compare palladium nanocubes with palladium on activated carbon, we have inverstigated to see that they exhibited the different chatacteristics in semi-hydrogenation. Palladium nanocubes having [100] facets represented substantially enhanced selectivity toward alkenes rather than the commercially available palladium on activated carbon enclosing [111], [110] and [100] facets did.

Key words: palladium nanoparticle, Pd nanocube, selective hydrogenation

Part II. Studies on the transition metals immobilized on multi-wall carbon nanotubes

Functionalization of multi-wall carbon nanotubes (MWNT) has been investigated using various methods. Among them, we selected nitrene chemistry as functionalization method to preserve peculiarities of MWNT. By using nitrene chemistry, we introduced various linkers such as amine, diamine, hydroxyl amine, and pyridine moieties on MWNTs, and then we tried to anchor transition metals on the linker-MWNT with reducing agents. After immobilization of transition metal, the metal with linker-MWNT played a role as a catalyst for various reactions such as nitro reduction. After the reaction, the used catalysts could be regained by centrifugation and drying, and they were reused for 10 times.

Key words: multi-wall carbon nanotube, functionalization, immobilization of transition metal, nitro reduction, recycle

List of Figures

Part I.

Part II.

Figure 1. Schematic presentation of the reaction of nitrenes with the nanotube sidewall

Figure 2 . TEM images of BMK-C704 with Pd

Figure 3. a) FT-IR, b) carbonyl group FT-IR, c) TGA data

Figure 4. a) H_2 bubbling 30 min, b) H_2 bubbling 1 h, c) H_2 bubbling 2 h, d) $NaBH_4$ 10wt%, e) $NaBH_4$ 25wt%, f) hydrazine monohydrate

Figure 5. a) $NaBH_4$, b) salt adding after H_2 bubbling, c) H_2 bubbling after salt adding

Figure 6. TEM and ICP data of each linker

List of Schemes

Part II.

List of Tables

Part I.

Part II.

Part I.

Studies on the shape-dependent catalytic activities of Pd nanoparticles

I. Introduction

Noble metal nanoparticles possessing unique properties are expected to be efficient catalysts for many organic reactions. Especially, various palladium nanoparticles can be employed in diverse reactions in the synthesis of fine chemicals as well as bulk chemicals in industry. In this regard, many catalytic applications utilizing Pd nanoparticles have been documented. [1-6]

There are many methods to improve the properties of Pd nanoparticles such as immobilization on various supporting groups,[7-9] synthesis of hybrid nanocrystals,[10, 11] exchange of metal sources and synthetic routes.[12,13] Some researchers have been interested in the studies of Pd nanoparticles to be used as chemoselective catalysts depending on their unique size or shape.[14,15] Selective reaction based on the size of Pd nanoparticle catalysts has been achieved.[16-19] Moreover, different planes of nanocrystal were shown to exhibit differences in catlaytic behaviors.[20-22] The differences in shape of Pd nanoparticles has been known to influence the reactivities.[23]

Many researchers have reported some catalysts for selective hydrogenation using low-active Raney nicel,[24] Ni-complex,[25] and homogeneous rhodium complexs.[26] However, these catalysts often suffer from a pyrophoric property, narrow substrate scope, and low cis-trans selectivity. For instance, Lindlar catalyst having palladium deposited on calcium carbonate is capable of selective hydrogenation of alkynes into alkenes,[27] but this method is limited only to the partial hydrogenation of di-substituted alkynes. Thus, the development of catalyst for the highly selective hydrogenation still remains to be a grand challenge.

Recently, Lioubov and Younan reported the structure sensitivity of reactions on shape- and size- controlled palladium nanocrystals. [28] They confirmed different activities and selectivities on the hydrogenation of

alkynols based on cubic, octahedral and cuboctahedral shapes. They had found that overhydrogenation occurs at edge sites and verified through kinetic modeling, but they only investigated the relationship between the selectivity and the proportion of low-coordination atoms in the surface of nanocrystals. In this paper, we initiated a systematic study on the selective hydrogenation of alkynes using Pd nanocubes enclosed by [100] facets and Pd on activated carbon having various facets such as [111], [110] and [100]. Comparing these two Pd source catalysts, we have identified that Pd nanocubes showed enhanced selectivity relative to Pd on activated carbon in the hydrogenation of various substrates having triple bond.

To prepare palladium cube nanoparticle, Na_2PdCl_4 was simply added into an aqueous solution containing poly(vinylpyrrolidone), L-ascorbic acid, and potassium bromide. Bromide ion played a role as a capping agent to synthesize Pd nanocubes having only [100] facets.

The Pd nanocubes showed good catalytic activities for reductions of carbon-carbon triple bonds to single bonds. We used gas chromatography (GC) to examine the amounts of both reactants and products. When the most of alkynes were converted into double bonds, single bonds started to appear, which suggested that selective partial hydrogenation of triple bond is possible (**Figure 1**).

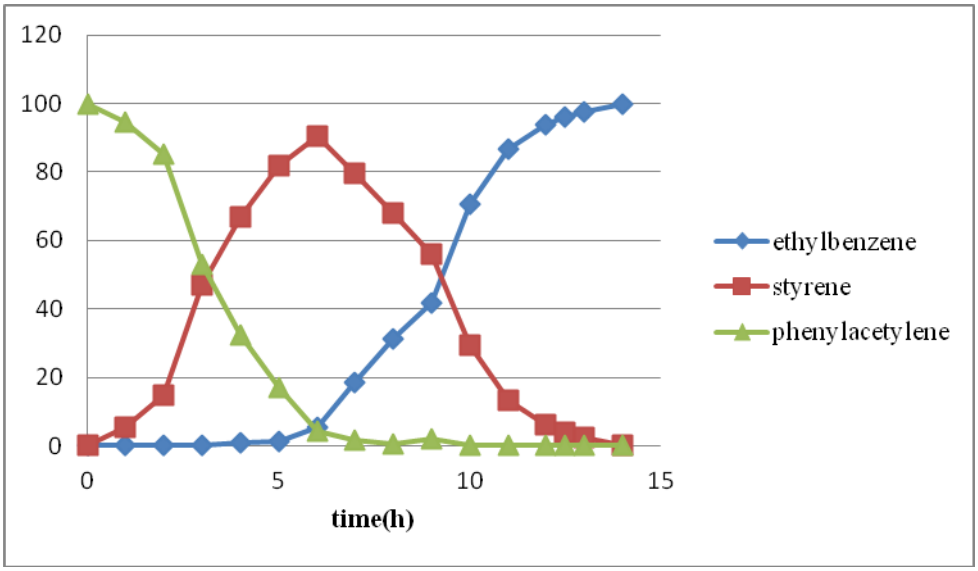

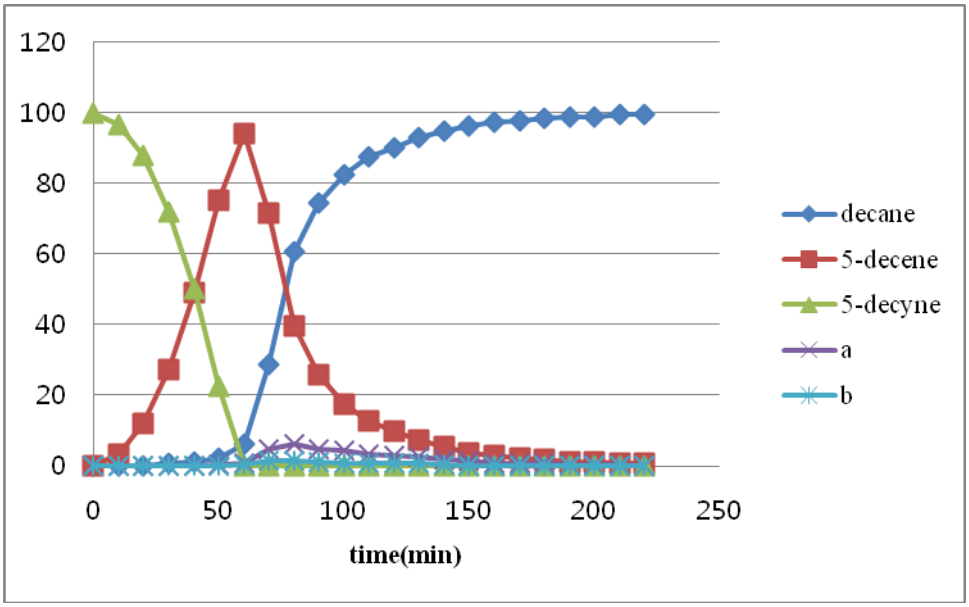

Figure 1. Hydrogenation pattern of a) phenyl acetylene and b) 5-decyne

II. Result and Discussion

At the starting point of the project, we used two types of palladium nanoparticles, octahedral and cubic. In hydrogenation, cube showed good selectivity in the production of double bond, whereas octahedral presented lower selectivity rather than cube shape of palladium (**Figure 2**). We then focused on the different shape-seletivities of palladium nanocubes.

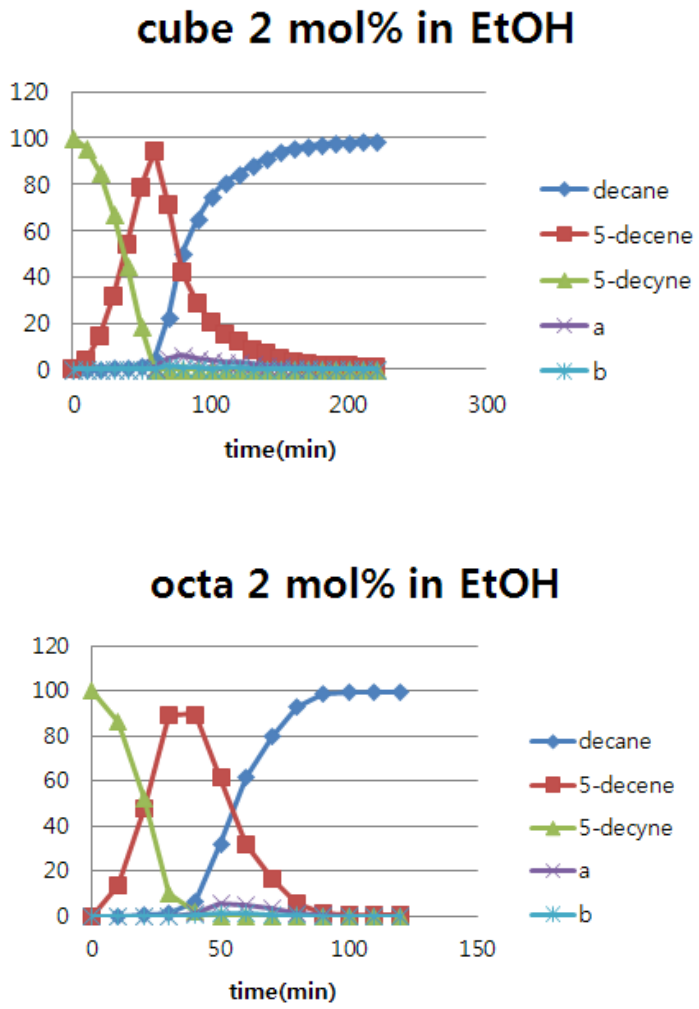

Figure 2. Hydrogenation of 5-deccyne a) Cube palladium nano particle, b) Octahedral nano particle

To compare reactivity between cube catalysts and commercially available palladium catalysts, we chose palladium on activated carbon (10wt%, Degussa type) as commercially available ones. Transmission electron microscopy (TEM) images to check the shape difference between Pd nanocubes and Palladium on activated carbon are shown in **Figure 3**. In **Figure 3a**, the nanocrystals were nearly 100% in cubic shape and had an average edge length of approximately 11 nm. The corresponding Fourier-transform (FT) pattern in **Figure 3b** reveals an array of spots with square symmetry, presenting that the Pd cube was a piece of single crystal bound by [100] facets. On the other hand, the TEM image of palladium on activated carbon indicates 3 nm-sized Pd nanocrystals with nearly spherical shape in **Figure 3c**. HRTEM image of Pd/C shows that nanocrystals are enclosed by various kinds of facets including [111], [110] and [100] facets in Figure 3d.

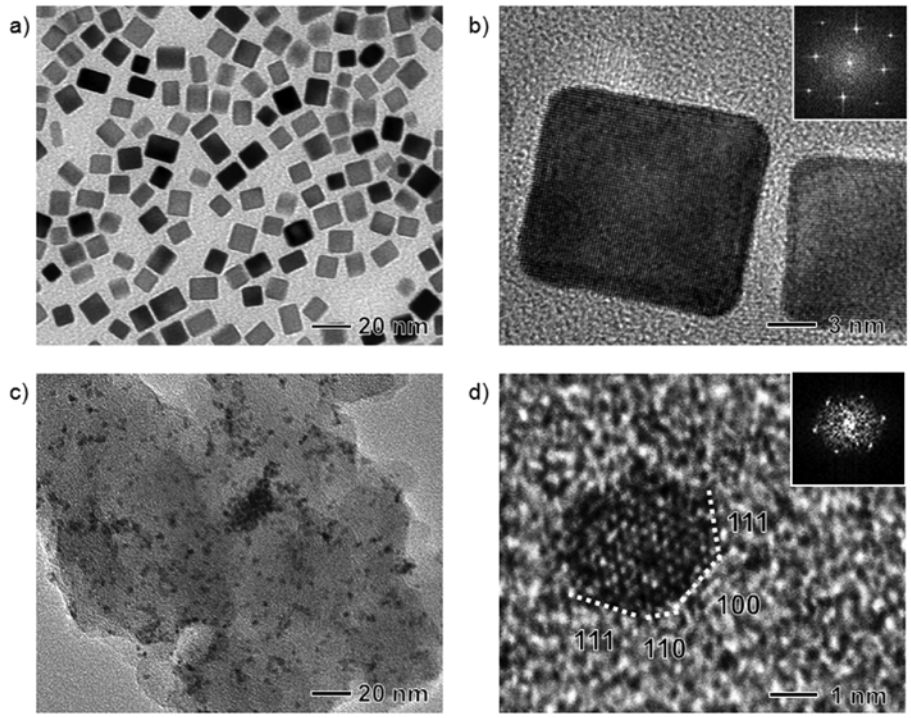

Figure 3. a) TEM and b) HRTEM images of Pd nanocubes, c) TEM and d) HRTEM images of commercial Pd/C. The insets show the corresponding FT patterns.

The catalytic properties of the two kinds of Palladium catalysts were evaluated by the hydrogenation of 5-decyne using hydrogen gas as a hydrogen source in an ethanol solution at room temperature. The reaction process was followed through GC analysis. **Figure 4a** shows a reaction pathway of the 5-decyne hydrogenation. In concequence, both Pd materials showed good reactivity for hydrogenation to decane from 5-decyne completely (**Figure 4**). Also, Pd nanocubes were much more effective in the selective production of olefins than palladium on activated carbon, even though the first reduction of 5-decyne in both cases was faster than the next hydrogenation of the resulting olefin.

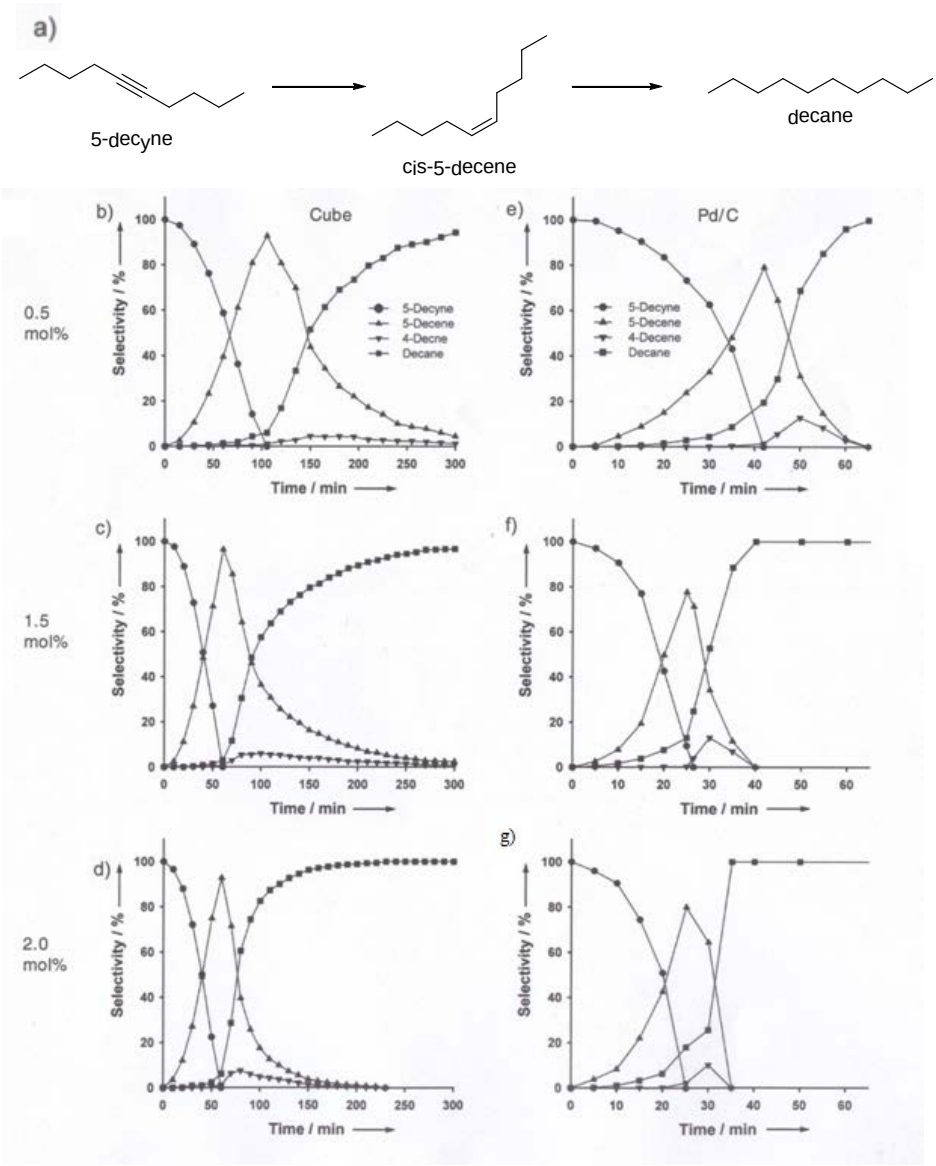

Figure 4. a) The scheme of 5-decyne hydrogenation. Evolution of hydrocarbon during 5-decyne hydrogenation with b) 0.5 mol% Pd cube, c) 1.5 mol% Pd, d) 2.0 mol% Pd cube, e) 0.5 mol% Pd/C, f) 1.5 mol% Pd/C, g) 2.0 mol% Pd/C.

According to the reaction time, the amount of partial hydoregenation product was evaluated through GC analysis and the data are shown in **Figure 5a**. The results of Pd on activated carbon and Pd nanocube, they represented different reduction patterns. Almost all starting material was converted into alkene in the 40% of overall reation time, and the rest of time was used in the conversion of alkene to alkane in the Pd nanocubes reaction. On the other hand, 70% of overall reaction time was required using palladium on activated carbon for partial hydrogenation. However, in Pd on activated carbon, before the triple bond conversion was complete, the reduction of olefins started to appear, which result in lower selectivity than Pd nanocube. Therefore, the partial hydrogenation of 5-decyne was relatively faster than the olefin reduction in the reactions using the Pd nanocubes and therefore chemoselective reduction of the alkyne was practically a viable process, which allows palladium nanocubes to be more selective hydrogenation catalyst rather than Pd/C. When 1.5 mol% of Pd catalysts were introduced, the selectivities of 5-decene were 96.4% for Pd nanocubes and 71.3% for commercial Pd/C, respectively, demonstrating that Pd nanocubes exhibited substantially enhanced selectivity relative to the commercial Pd/C catalysts (**Figure 5b**). In this research, we accomplished selective formation of pure cis-5-decene at the time when reactant was fully consumed. To achieve a better understanding of the effect between selectivity and the amount of Pd catalyst, we confirmed that Pd nanocubes maintained high selectivity in all range of concentration of Pd catalysts (**Figure 5c**). It is worth pointing out that the total reaction rate of Pd nanocubes was slower than that of the commercial Pd/C presumably because particle size of Pd/C is smaller than nanocubes so that catalytic surface area of the commercial Pd/C is larger compared with Pd nanocubes.

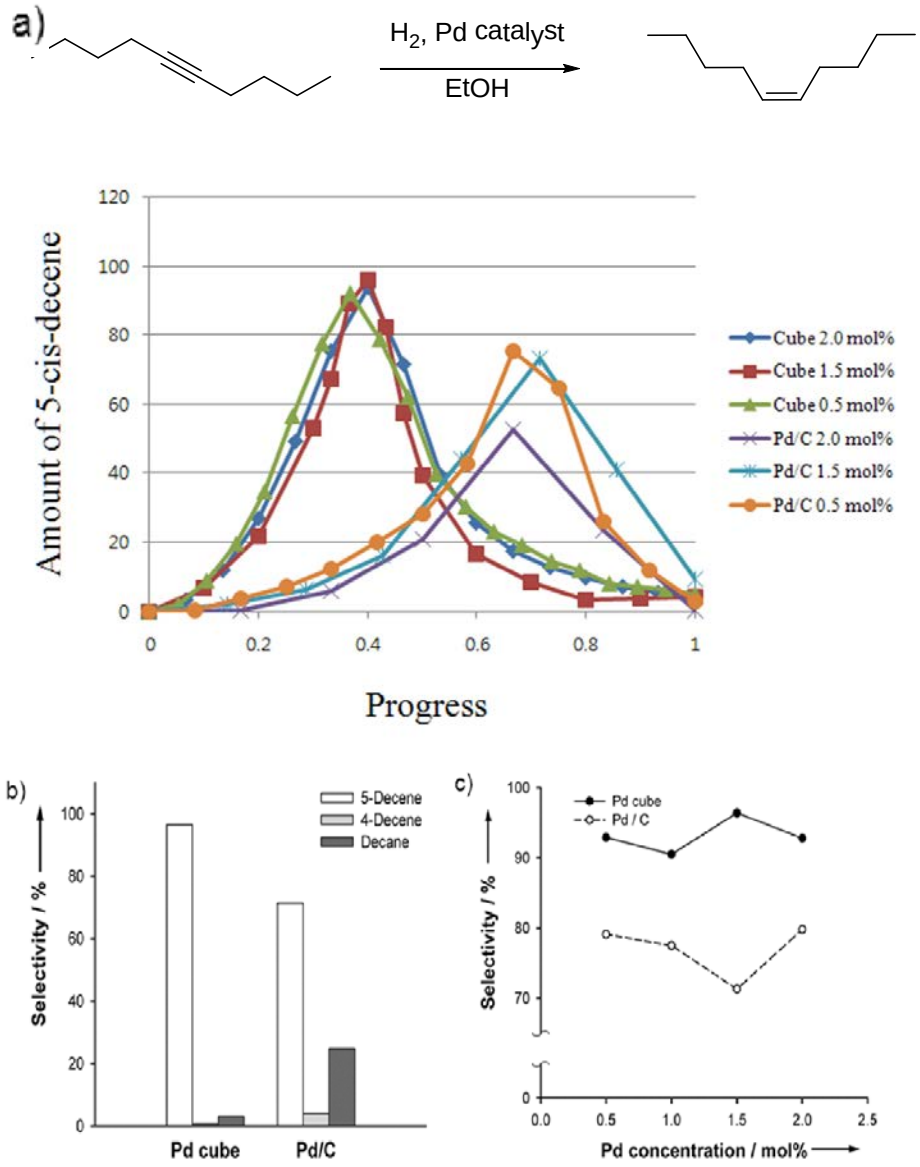

Figure 5. a) The amount of the semihydrogenation products according to progress (time). b) Product distribution of the various Pd catalysts. c) The selectivities toward 5-decene in different concentrations of Pd catalysts (0.5, 1.0, 1.5 and 2.0 mol%).

To identify this selective characteristic of Pd nanocube, we carried out semihydrogenation of various alkyne substrates and the results are summarized in **Table 1**.

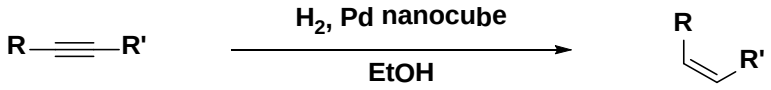

Entry	Substrate	Product	triple	double	single
1	1-octyne	1-octene	6.7	91.5	1.7
2	1-decyne	1-decene	0.6	83.9	11.5
3	2-decyne	*cis*-2-decene	2.0	86.6	4.3
4	3-decyne	*cis*-3-decene	1.9	88	2.1
5	4-decyne	*cis*-4-decene	6.7	91.6	1.2
6	5-decyne	*cis*-5-decene	1.5	95.0	3.1
7	phenyl acetylene	styrene	4.3	90.3	5.4
8	2-butyne-1,4-diol	2-butene-1,4-diol	0	97.9	2.1
9	Diethylacetylene-di carboxaldehyde	diethylmaleate	12.8	79.7	7.5

- All the reactions were carried out with 1.0 mmol of alkyne and 1.0 mol% Pd nanocubes in 2 mL of EtOH. The yields are determined by GC.

Table 1. Semihydrogenation of alkynes using Pd nanocubes

Regardless of the location of the triple bond, the reaction of internal alkyne and terminal alkyne proceeded smoothly. (**Entries 1-6**) Even in the presence of other functional groups, the triple bond was reduced selectively. (**Entries 7-9**)

After the catalytic reaction, Pd nanocubes were collected by centrifugation, redispersed in water, and then characterized by TEM in order to confirm the morphological stability of the catalysts during the reaction. **Figure 6** shows the TEM images of Pd nanocubes after catalytic reaction, indicating that the Pd catalysts maintained their cubic shape.

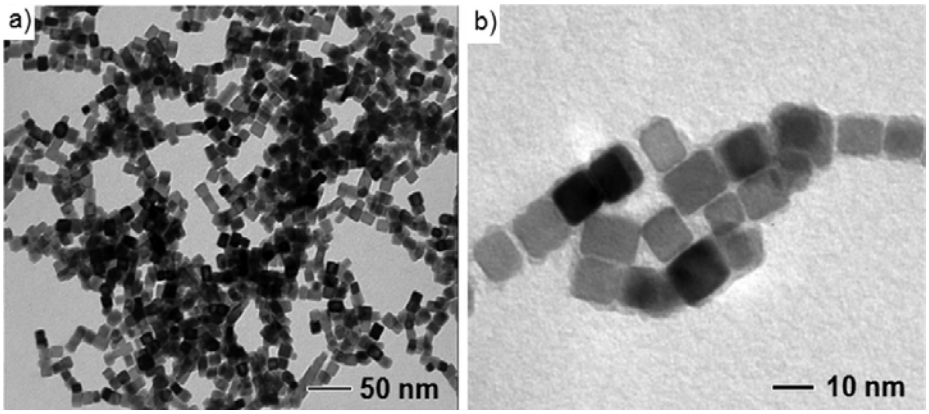

Figure 6. TEM images of Pd nanocubes after 5-decyne hydrogenation.

III. Conclusion

In conclusion, we have investigated a chemoselective catalytic system for hydrogenation of alkynes into alkenes over palladium nanocubes. Pd nanocubes having [100] facets exhibited enhanced selectivity toward alkenes compared with the palladium on activated carbon which has spherical Pd nanocrystals enclosed by various facets, [111], [110], and [100]. Even though many selective catalytic studies for selective partial hydrogenation have already been reported such as poisoning agents,[29] our results clearly demonstrate that the Pd nanocrystals with fine-controlled shapes can be considered as a good candidate for catlaysts with high selectivities maintaining stability and ease of catalyst recovery.

IV. Experimental

Synthesis of Pd nanocubes

In a typical synthesis of Pd nanocubes, 11 mL of an aqueous solution containing poly(vinyl pyrrolidone) (105 mg), L-ascorbic acid (60 mg), KBr (200 mg), and Na_2PdCl_4 (57 mg) was stirred at 80° C in air under magnetic stirring for 3 h and cooled down to room temperature. After cooling, the mixture was gathered by centrifugation, washed with water and dried under vaccum oven.

A General Procedure for hydrogenation using Palladium catalyst

To an oven-dried, 5 mL round-bottom flask, magnetic stir bar was equipped. Then Palladium catalyst and degassed ethanol (2.0 mL) were added to the flask, and the mixture was sonicated in an ultrasonic bath for 10 min. After sonication, a substrate (0.40 mmol) was added to the flask and the mixture was stirred at room temperature under hydrogen atmosphere. The course of the reaction was periodically followed by stopping the stirring and taking aliquots (10μL) which were analyzed through GC. All the products were characterized by comparison with pure samples.

Part II.

Studies on the transition metals immobilized on multi-wall carbon nanotubes

I. Introduction

Carbon nanotubes (CNTs) have attracted much interest in recent years because of their electronic, mechanical and structural properties.[1] These special properties make CNTs very useful for supporting metal nanoparticles in many potential applications. Many researchers have focused on creating rational methods to functionalize CNTs.[2,3] Modified CNTs can be applied to molecular electronics, biological sensors, catalyst support, superior sorbent, and polymer composites.[4] There are two strategies to modify CNTs; noncovalent functionalization and covalent functionalization. Noncovalent functionalization of CNTs has been extensively researched to fill novel individual crystals in the inerior of CNTs to oppose to defect-site and covalent-sidewall functionalization, which helps conservation of electronic structure of CNTs by preventing disruption of the intrinsic nanotube sp^2 structure and conjugation. On the other hand, covalent functionalization of CNTs has a good chance to solubilize and disperse in a variety of solvents and leads to the creation of novel composite materials although covalent interaction with the surfaces of CNTs may cause defects from chemical functionalzation.[5,6] Researchers have reported various methods to modify CNTs. Among them, commonly used direct and covalent modification of CNT sidewall methodologies can be summarized as shown in Table 1.[6]

Table 1. Common CNT sidewall functionalization methods.

Method	Addend	Degree of functionalization	Solubility
Diazonium[5]	Aryl	1 addend/ 10 carbon	0.8 mg / mL in DMF
Diazonium in oleum[6]	Aryl	1 addend /20 carbons	0.25 mg / mL in H2O
Fluorination[7]	Fluorine	1 addend / 2 carbons	1 mg / mL in 2-propanol
Radical chemistry[8]	Alkyl	1 addend / 6 carbons	-
Dissolving metal reduction[9]	Alkyl, aryl	1 addend / 17 carbons	-
Azomethine ylide (Prato reaction)[10]	Pyrrolidine	1 addend / 100 carbons	50 mg / mL in DCM
Nitrene[11]	Aziridine	1 addend / 50 carbons	1.2 mg / mL in DMSO
Bingel reaction[12]	Cyclopropane	1 addend / 50 carbons	-
Dichlorocarbene[13]	Cyclopropane	1 addend / 25 carbons	-

All our works on CNT were carried out using multi-walled nanotube (MWNT) prepared by chemical vapor deposition (CVD) method. There are many different features between single and multi-wall nanotubes, but we initiated our research based on a simple assumption that functionalization method for single-wall nanotube (SWNT) can be applied to MWNT.

In order to make functionalized CNTs, we attempted to modify the sidewall of MWNT with covalent bonds using several functionalization methods.

For this purpose, we carried out diverse reactions with azido linker to attach functional groups and fixed transition metals on MCNTs for use in catalytic systems. (**scheme 1**)

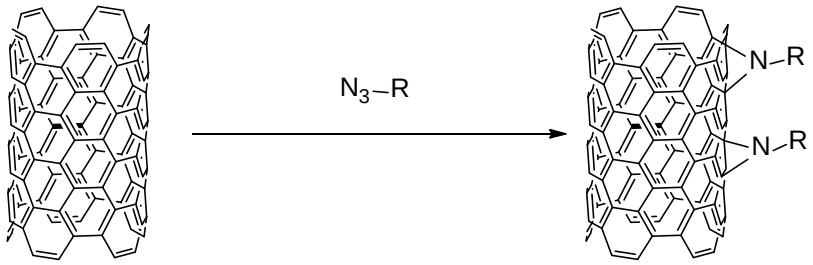

Sheme 1. Aziridine functionalized MWNT

II. Result and Discussion

- Functionalization of MWNT

We chose nitrene chemistry as a functionalization mothod. Nitrenes are uncharged, electron deficient molecular species. Therefore, generated nitrenes can add, insert or rearrange by using reactive imtermediate generally formed *in situ* from an azide. Singlet-state and triplet-state nitrenes are generated after thermal or light-induced extrusion of N_2. The singlet-nitrenes that have two p-orbitals, each filled with two electrons, can either attack the nanotube sidewall in an electrophilic [2+1] cycloaddtion or undergo a transition into a triplet-state by inter-system crossing. Triplet-state nitrenes that have one filled p-orbital and two p-orbitals with un-paired electrons are biradicals with un-paired electrons, which allows them to react with the π-system of the nanotube sidewalls. In both cases, aziridine rings can be formed (**Figure 1**).

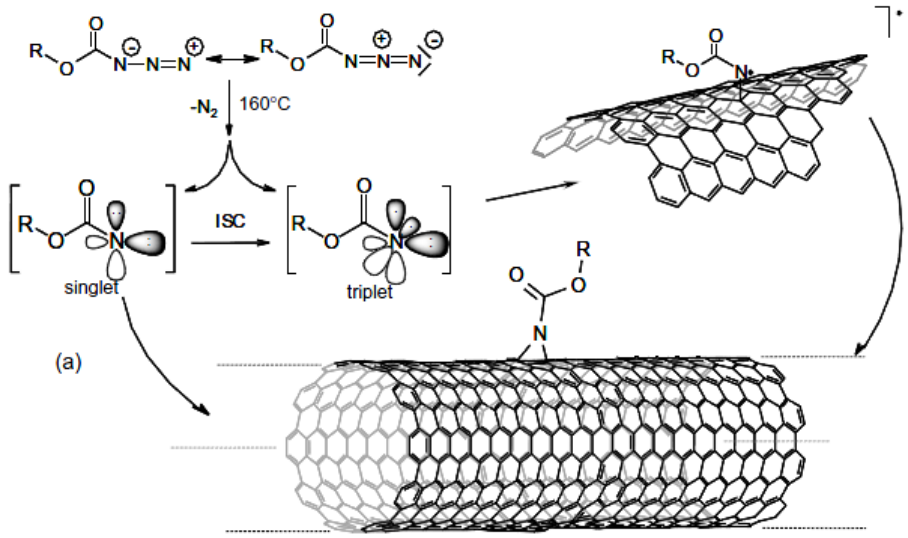

Figure 1. Schematic presentation of the reaction of nitrenes with the nanotube sidewall.[12]

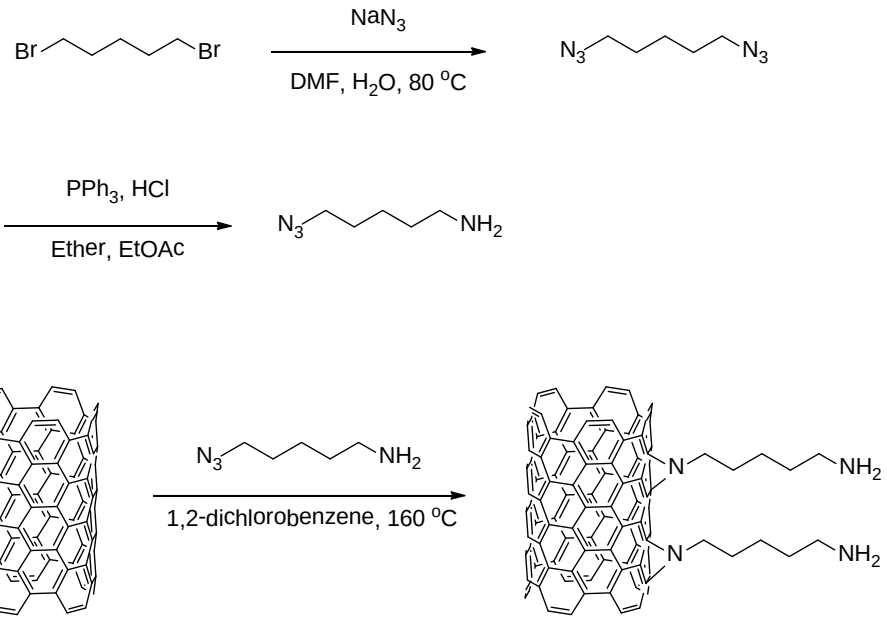

Scheme 2. Synthesis of BMK-C704 and MWNT functionalization

Following in most reports dealing with the nitrene chemistry,[8-10] we attempted to use amino alkyl azide for CNT functionalization for the nitrene chemistry.

Each 100 mg of MWNT was treated with 200 wt% of 5-azidopentylamine in 1,2-dichlorobenzene to generate an amine anchored-MWNT, BMK-C704. Functionalized MWNT changed its dispersibility. To use this MWNT, we tried to immobilize palladium on it through reduction with hydrogen gas.

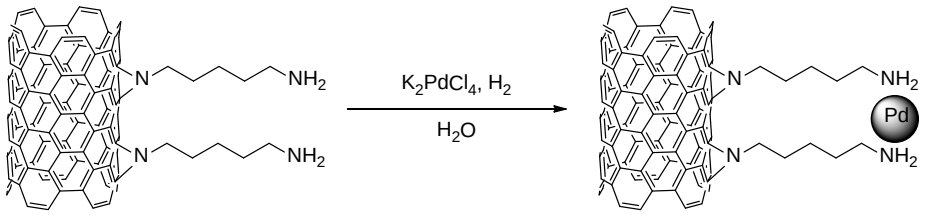

Scheme 3. Palladium loading on BMK-C704

Using ICP-MS, we found that 13.0 wt% of the Pd-amine-CNT (BMK-C704 with Pd) consisted of palladium metal. We tested hydrogenation reaction of phenyl acetylene by using 1 mol% of Pd catalyst. After reaction was complete, the catalyst was recovered by centrifugation and dried under vacuum oven and reused for recyling reaction. Result of recycling experiment is summarized in **Table 2**.

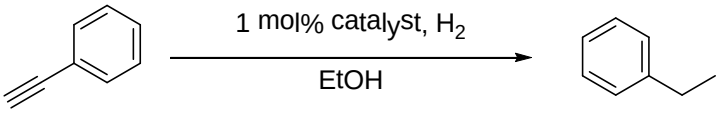

Run	1st	2nd	3rd	4th	5th	6th	7th
Time (min)	180	90	60	30	30	60	270
Conversion (%)[a]	99	99	99	99	99	99	99

a. Yields were determined by GC analysis

Table 2. Recycle test of BMK-c704 with palladium catalyst.

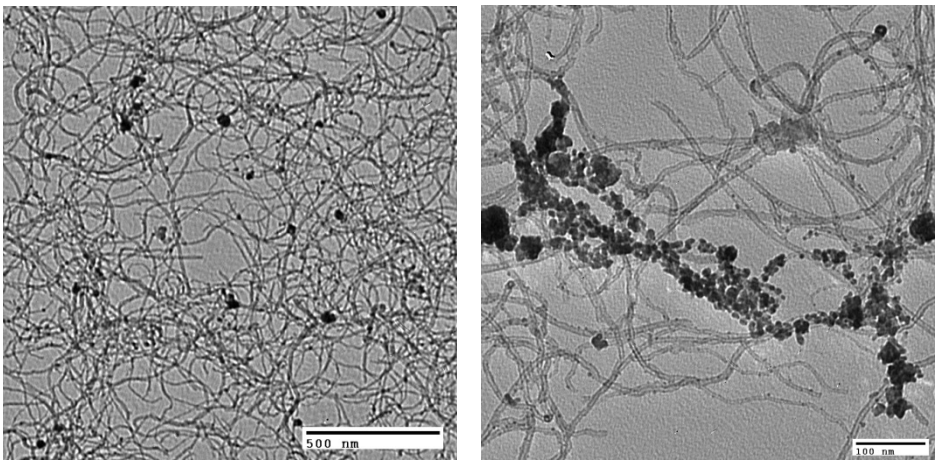

Figure 2. TEM images of BMK-C704 with Pd

At first reaction, BMK-C704 with Pd showed excellent catalytic activity in hydrogenation. However, upon recycling, the catalytic activity of BMK-C704 with Pd decreased due to leaching out of Pd. Also, we confirmed that the immobilization of palladium of the MWNT was not uniform through TEM (**Figure 2**).

To solve these problems, we decided to modify azido-linkers that have better ligating ability comtaining more oxygen or nitrogen to catch metal. Moreover, we introduced various reduction agents to load transition metals to immobilize uniformly on the surface of MWNT.

We modified the linker with pyridine moiety from BMK-C704 as shown in scheme 4.[10]

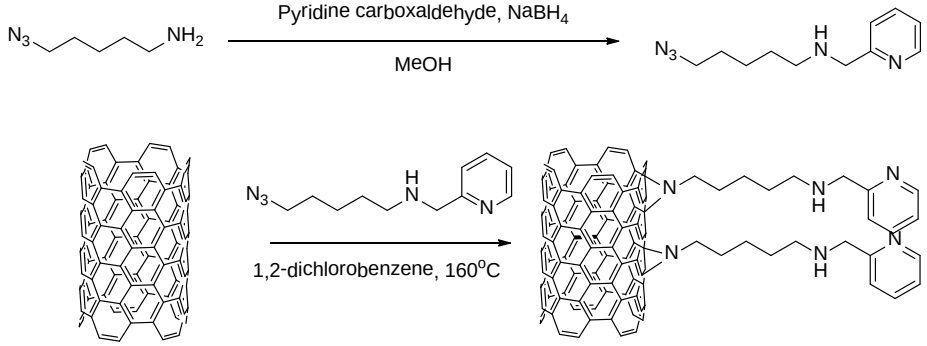

Scheme 4. Synthesis of the pyridine containing linker and functionalization of MWNT

Also, we designed the linkers with more heteroatoms such as nitrogen and oxygen to ensure tighter binding to metals (scheme 5).[11,12] The carbonyl group in the linker allowed us to follow the process in each step through IR analysis.

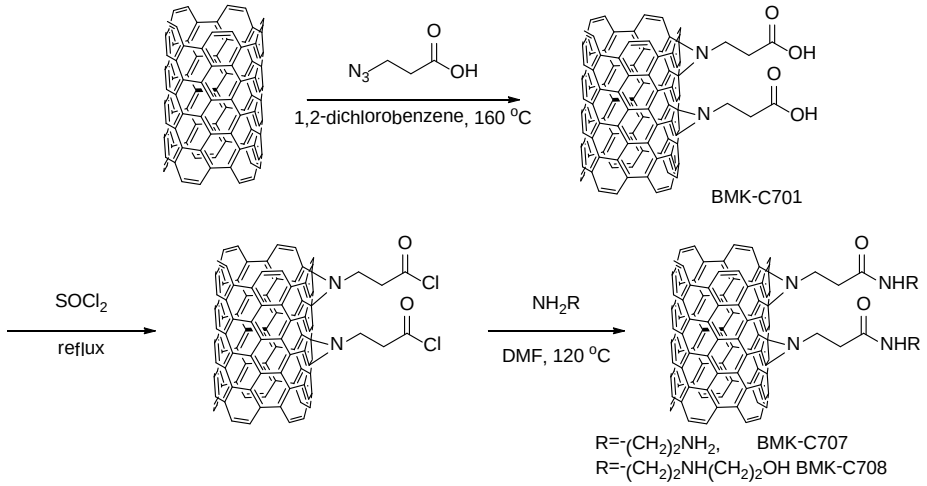

Scheme 5. Synthesis of BMK-C707 and 708 linkers

Functionalized MWNTs were confirmed by IR, EA and TGA (**Table 3 & Figure 3**).

	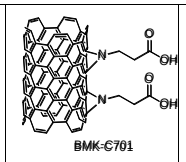 BMK-C701	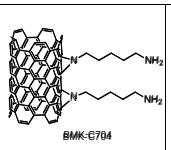 BMK-C704	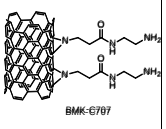 BMK-C707	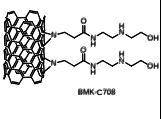 BMK-C708	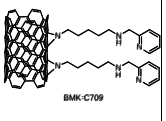 BMK-C709
EA	4.00 mmol	1.20 mmol	2.90 mmol	1.80 mmol	0.50 mmol
TGA[a]	6.20 mmol	1.10 mmol	2.87 mmol	1.66 mmol	0.49 mmol

a. The molecular weight change between 280 ^{o}C and 400 ^{o}C

Table 3. The amount molecular weight by EA and TGA

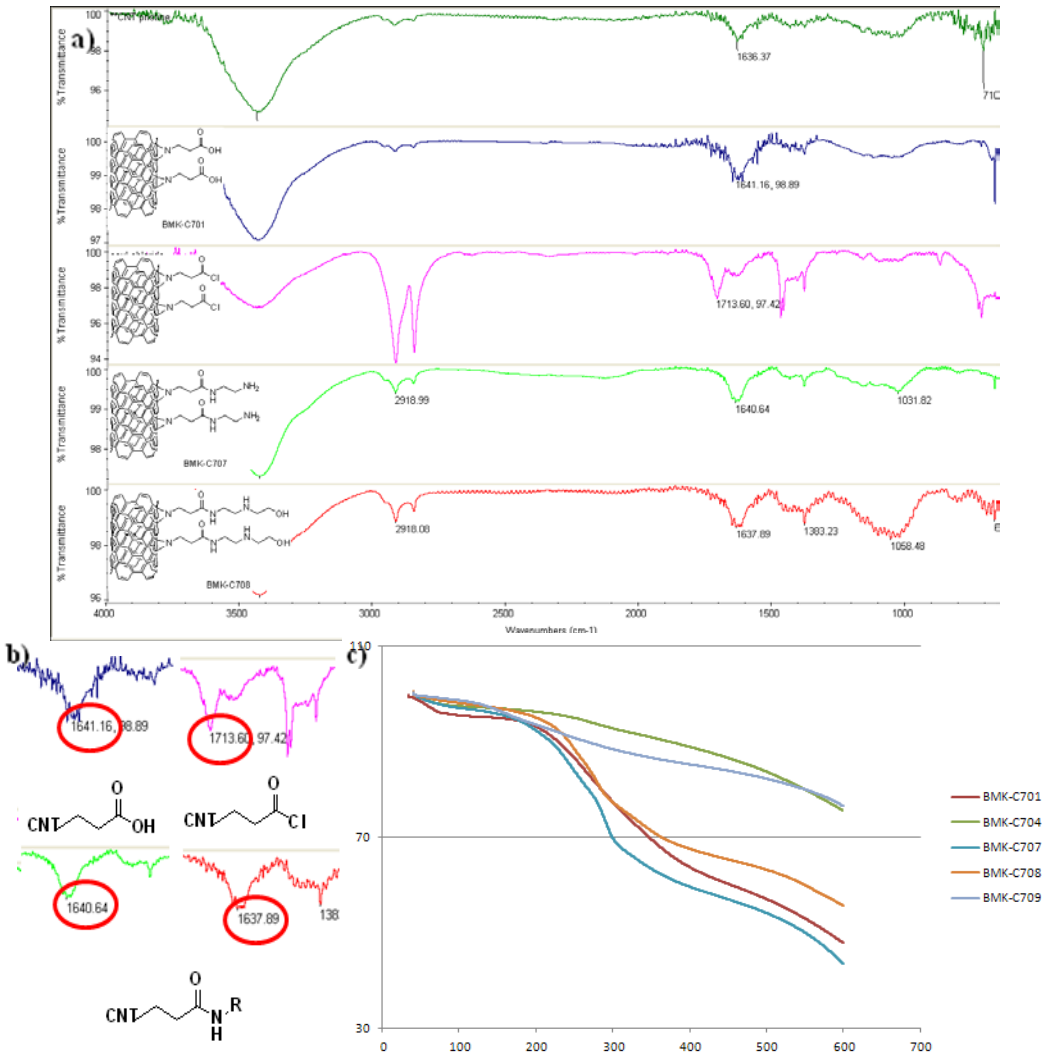

Figure 3. a) FT-IR, b) carbonyl group FT-IR, c) TGA data

- **Immobilization of a metal**

As mentioned earlier, we fixed palladium on the MWNT using hydrogen bubbling. Even though BMK-C705 had enough palladium to make use of catalyst, palladium was loaded partially on MWNT and leached out after reaction. Then we tried to apply various reducing agents such as hydrogen gas and sodium borohydride to immobilize palladium (**Figure 4**).

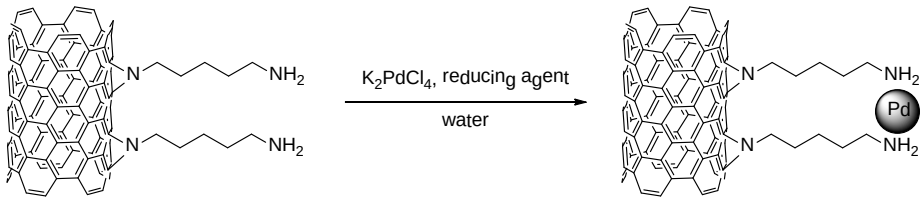

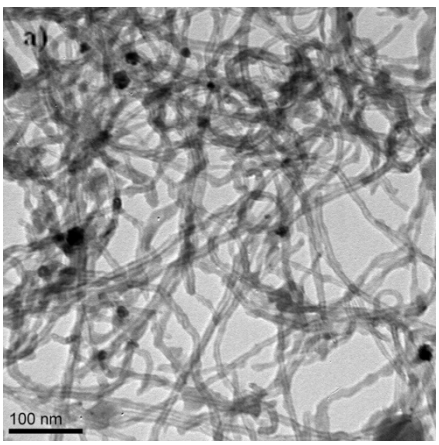

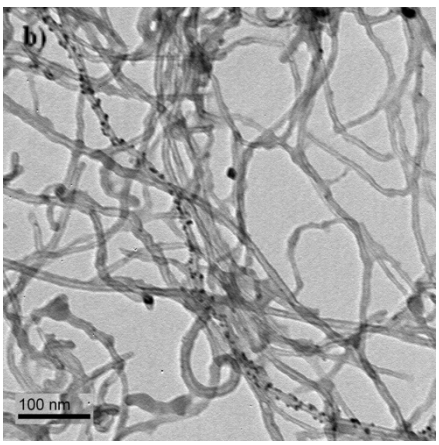

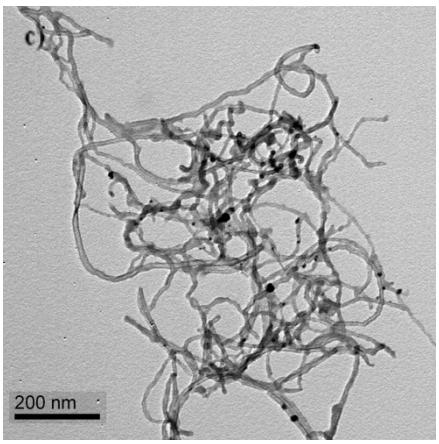

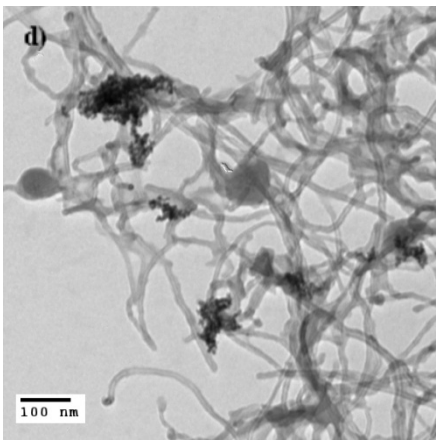

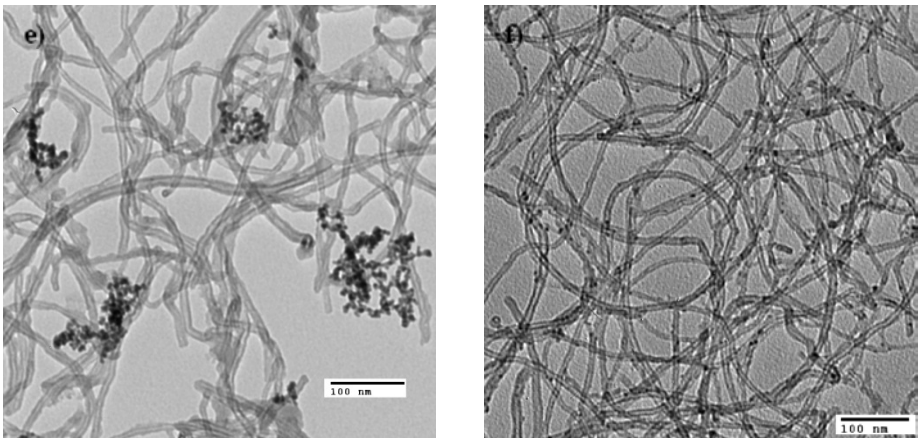

	a	b	c	d	e	f
ICP data	9.78wt%	13.0wt%	6.38wt%	11.2wt%	10.2wt%	14.0wt%

Figure 4. a) H_2 bubbling 30min, b) H_2 bubbling 1h, c) H_2 bubbling 2h, d) $NaBH_4$ 10wt%, e) $NaBH_4$ 25wt%, f) hydrazine monohydrate

The palladium loading with hydrogen gas or sodium borohydride resulted in metal on MWNT fixed irregularly as shown in TEM data. On the other hand, we introduced hydrazine monohydrate for immobilizing palladium, which allowed us to load palladium uniformly as shown in **Figure 3-f**.

Platinum has higher reduction potential than palladium, so it may require more powerful reducing agent. Shown in **Figure 5**, platinum with hydrogen gas was better loaded than using sodium borohydride.

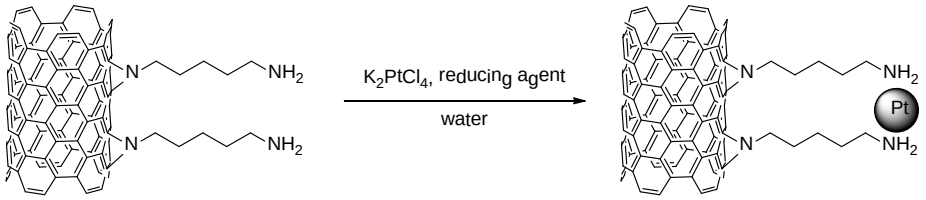

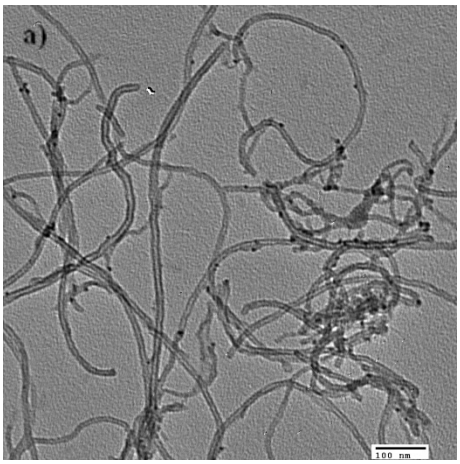

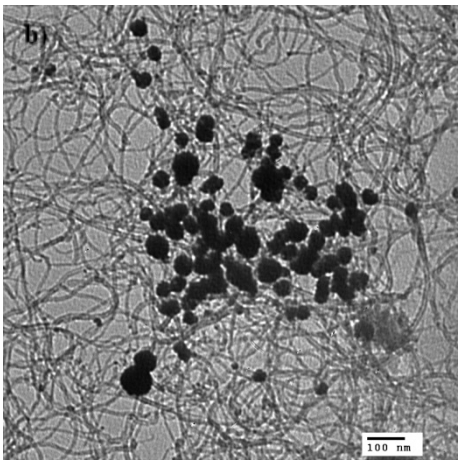

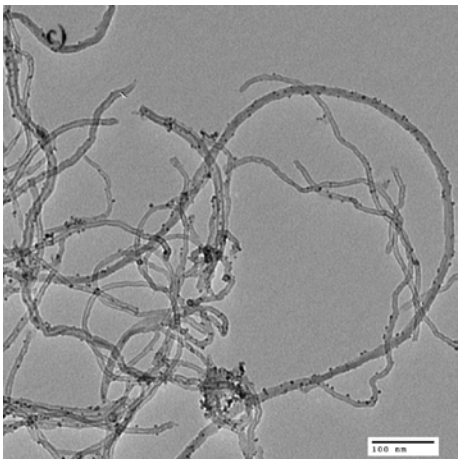

	a	b	c
ICP data	5.25wt%	11.4wt%	12.4wt%

Figure 5. a) $NaBH_4$, b) salt adding after H_2 bubbling, c) H_2 bubbling after salt adding

We applied metal two different loading methods, palladium with hydrazine and platinum with hydrogen gas, into each MWNT with different linkers. (**Figure 6**)

	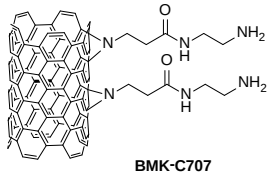 BMK-C707	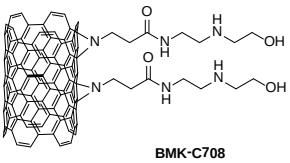 BMK-C708	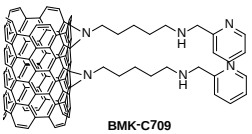 BMK-C709
Pd	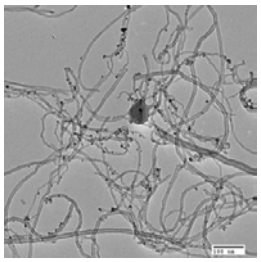	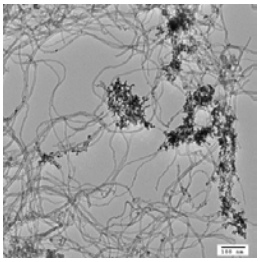	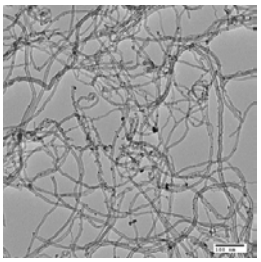
Pt	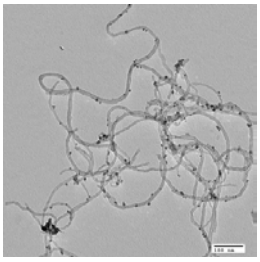	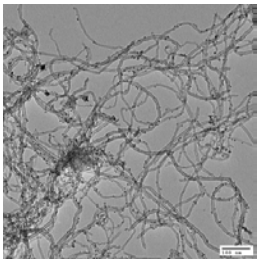	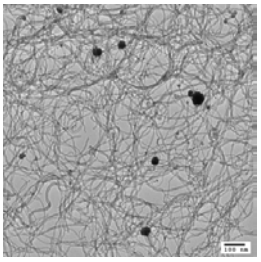
ICP-mass	Pd- 17.1wt% Pt- 22.5wt%	Pd- 12.0wt% Pt- 18.3wt%	Pd- 12.1wt% Pt- 16.0wt%

Figure 6. TEM and ICP data of each linker

Pyridine-containing linker (BMK-C709) with metal was not spread evenly, whereasregularly sized metals were ditstributed in BMK-C707 and 708.

We carried out reduction of nitro-functional gropus with these Pt-CNT-linkers. Even though BMK-C709 showed poor reactivity, we confirmed that platinium catalysts with BMK-C707 and 708 have good reactivity towards the nitro-reduction. After 10th recycle tests, catalytic activity decreased. This is presumally due to the fact that the amount of loading metal was leached out in repeatedly reaction.

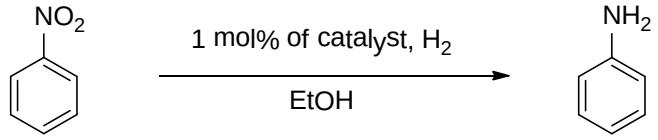

	1st	2nd ~ 10th	11th
BMK-C707 with Pt	99.9% (3h)	99.9% (3h)	76.4% (3h)
BMK-C708 with Pt	99.9% (2h)	99.9% (2h)	88.9% (2h)
BMK-C709 with Pt	99.9% (8h)	99.9%(10h)	

Yields were determined by GC analysis

Table 4. Recyle data with the nitroreduction scheme

III. Conclusion

We selected the nitrene chemistry to functionalize MWNT surface and made use of the resulting material as a new support for transition metal catalysts. Catalysts prepared from the above experiments showed excellent reactivity in hydrogenation. However, palladium was not immobilized and leached out in repetitive catalytic reactions. To solve these problems, we prepared other linkers to hold the metal much stronger than a single primary amine linkers do. Also, we tried to develop methods to immobilize metal using various reducing agents. These new catalytic systems showed the good distribution of metal on the functionalized MWNT and we were able to peform recycle experiments over 10 times in the reduction of nitro-compounds. Now, we are in the process of searching for new reactions to apply these catalytic systems.

IV. Experimental

Preparation of linkers

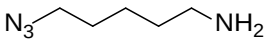

Sodium azide (2.54 g, 39.1 mmol) was added to dibromopentane (3.00 g 13.1 mmol) in 65.2 mL of dimethylforamide (DMF). After water (6.52 mL) was added, mixture was heated at 80 ^{o}C and stirred overnight. The resulting solution was concentrated *in vacuo* for the removal of DMF. The mixture was mixed with water and extracted with dichloromethane (3 x 65 mL). Combined organic layers were dried over sodium sulfate, filtered, and concentrated under reduced pressure. Diazidopentnae (1.75 g, 11.4 mmol, 87.0% yield) was obtanied.

Diazidopentane (1.75 g, 11.4 mmol) was soluted in 37.8 mL of ether and 37.8 mL of 2N HCl. Triphenyl phosphine (2.83 g, 10.8 mmol) in 37.8 mL of ethyl acetate was added slowly at 0 ^{o}C. After stirring at room temperature for 12 h, the reaction mixture was concentrated *in vacuo* for the removal of ether and ethyl acetate. The mixture was extracted with dichloromethane (3 x 40 mL). Sodium bicarbonate solution was added into water layer at 0 ^{o}C until pH 9. The reaction mixture was extracted with ethyl acetate (3 x 60 mL). Combined organic layers were dried over sodium sulfate, filtered, and concentrated under reduced pressure. Product (1.03 g, 8.13 mmol, 71.3% yield) was obtained.

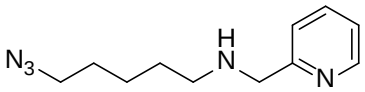

To a solution of 2-pyridine carboxaldehyde (0.819 g, 7.60 mmol) and 5-azidopentylamine (1.00 g, 7.80 mmol) in 26.0 mL of methanol was added

sodium borohydride (295 mg, 7.8 mmol) slowly at 0 ^{o}C. Then, the mixture was warmed up to room temperature and stirred overnight. Water (26.0 mL) was added to the mixture and methanol was removed by evaporation. Aqueous layer was then extracted with ethyl acetate (3 x 30 mL) and the combined extracts were dried over $MgSO_4$. After concentration, the residue was purified by chromatography on silica gel to give brownish oil (1.42 g, 6.51 mmol, 83.4% yield).

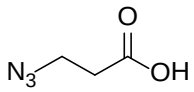

3-bromopropionic acid (3.00 g, 19.6 mmol) was dissolved in acetonitrile (31.6 mL) and sodium azide (2.57 g, 39.5 mmol) was added to the solution, the mixture was refluxed for 4 h. Acetonitrile was removed *in vacuo* and the resulting residue was suspended in 32 mL of ethyl acetate and extracted with 0.1 N HCl (2 x 30 mL), water (2 x 30 mL) and brine (2 x 30 mL). The organic layer was dried with sodium sulfate to afford 3-azidopropionic acid(1.98 g, 17.2 mmol) in 87.0% yield.

Preparation of Amine-CNT using nitrene chemistry

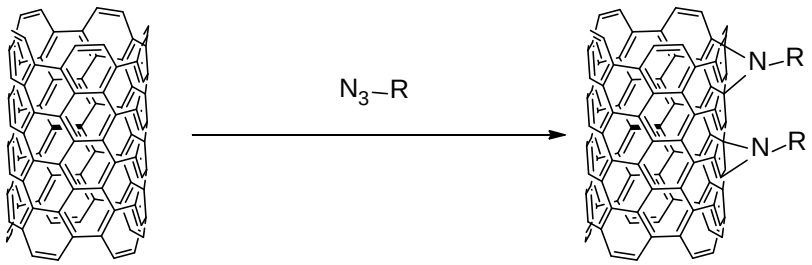

To an oven-dried 500 mL beaker, 100 mg of MWNT was charged then dispersed in 200 mL of 1,2-dichlorobenzene. The dispersion was sonicated with tip sonicator for 60 min (20 min x 3), transferred to 500 mL two-necked rbf, bubbled with argon gas for 10 min then heated to 160 ^{o}C.

After 30 min, 5-azidopentrylamine (1.00 g) was dissolved in 10 mL of 1,2-dichlorobenzene, and slowly added to the dispersion of MWNT (4 mL/h). The reaction mixture was allowed to stir at 160 ^{o}C for 16 h, then cooled to r.t, poured into 200 mL of THF. Black-colored MWNT pad (193 mg) was obtained by filtration, washing and drying in vacuum oven.

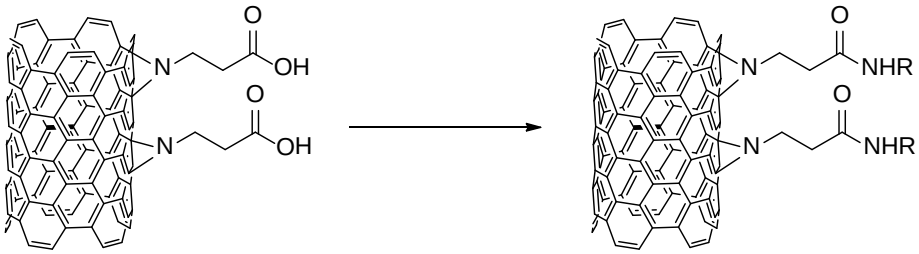

R=-$(CH_2)_2NH_2$,
R=-$(CH_2)_2NH(CH_2)_2OH$

To an oven-dried 250 mL rbf, 100 mg of BMK-C701 was dispersed in 20 mL of thionyl chloride and sonicated for 1h. After sonication, the mixure was bublled with argon gas for 10 min then reflux overnight. The reaction mixture was evaporated to remove thionyl chloride, THF was added, and evaporated again to get rid of residue thionyl chloride.

200 mL of DMF was added and sonicated for 1h, then was stirred at 120 ^{o}C. After 10 min, 1 mL of ethylene diamine or N-(2-hydroxyethyl)ethylene diamine was slowly added and stirred at 120 ^{o}C. After 12h, the mixture was cooled to room temperature, filtered, washed with water and THF, and dried in vacuum oven at 70 ^{o}C for 12 h.

Preparation of Pd-Amine-CNT with hydrazine monohydrate

To an oven-dried 500 mL beaker, 100 mg of MWNT was charged then dispersed in 200 mL of distilled water, then sonicated with tip sonicator for 60 min (20 min x 3). The dispersion was transferred to 500 mL two-necked rbf

and bubbled with argon gas for 10 min, then K_2PdCl_4 (50 mg) was dissolved in 10 mL water, then slowly added into rbf. The reaction mixture was bubbled with argon gas for 10 min again and heated 80 ^oC. After 10min, 10 mL of hydrazine was slowly added (4 mL/h) and stirred under argon gas (1 atm) for another 12 h. The mixture was poured into 200 mL of THF. Black precipitate was gathered by filtration, washed with water and THF, and then dried in vacuum oven at 70 ^oC for 12 h.

Preparation of Pt-Amine-CNT with hydrogen gas bubbling

To an oven-dried 500 mL beaker, 100 mg of MWNT was charged then dispersed in 200 mL of distilled water, then sonicated with tip sonicator for 60 min (20 min x 3). The dispersion was transferred to 500 mL two-necked rbf, then K_2PtCl_4 (50 mg) was dissolved in 10 mL water, then slowly added into rbf. The reaction mixture was bubbled with hydrogen gas for 1 h. The resulting mixture was allowed to stir under hydrogen gas (1 atm) for another 12 h. The mixture was poured into 200 mL of THF. Black precipitate was gathered by filtration and then was washed with water and THF, and then dried in vacuum oven at 70 ^oC for 12 h.

Representative procedure of nitro-reduction Pt-functionalized MWNT

Pt-linker-CNT (1 mol%) was charged in a 10 mL two-necked rbf then 5 mL of ethyl alcohol was injected. Nitrobenzene (51.3 μL, 0.5 mmol) was added and degassed with argon gas for 10 min. The mixture was sonicated for 10 min and stirred under 1atm hydrogen gas. After reaction over, the reaction mixture was transferred to 15 mL conical tube. Pt-linker-CNT was gathered by centrifugation (6000 rpm, 10min) then washed with THF and dried under vacuum oven. Dried Pd-Amine-CNT was transferred to 10 mL two-necked rbf, and involved in the next cycle of the reaction.

Reference

Part I

1. H. Ohde, C. M. Wai, H. Kim, J. Kim, M. Ohde, *J. Am. Chem. Soc.* **2002**, *124*, 4540-4541.

2. Y. Jiang, Q. Gao, *J. Am. Chem. Soc.* **2006**, *128*, 716-717.

3. N. Kim, M. S. Kwon, C. M. Park, J. Park, *Tetrahedron Lett.* **2004**, *45*, 7057-7059.

4. K. Okamoto, R. Akiyama, H. Yoshida, T. Yoshida, S. Kobayashi, *J. Am. Chem. Soc.* **2005**, *127*, 2125-2135.

5. N. Semagina, E. Joannet, S. Parra, E. Sulman, A. Renken, L. Kiwi-Minsker, *Applied Catalysis A: General* **2005**, *280*, 141-147.

6. S. Kidambi, J. Dai, J. Li, M. L. Bruening, *J. Am. Chem. Soc.* **2004**, *126*, 2658-2659.

7. J. Park, C. Park, M. Kwon, *Synthesis* **2006**, *2006*, 3790-3794.

8. S. Mori, T. Ohkubo, T. Ikawa, A. Kume, T. Maegawa, Y. Monguchi, H. Sajiki, *J. Mol. Catal. A: Chem.* **2009**, *307*, 77-87.

9. A. Corma, H. Garcia, A. Leyva, *J. Mol. Catal. A: Chem.* **2005**, *230*, 97-105.

10. W.-J. Kim, S. H. Moon, *Catal. Today* **2011**.

11. Y. Jang, J. Chung, S. Kim, S. W. Jun, B. H. Kim, D. W. Lee, B. M. Kim, T. Hyeon, *Phys Chem Chem Phys* **2011**, *13*, 2512-2516.

12. Á. Mastalir, Z. Király, *J. Catal.* **2003**, *220*, 372-381.

13. R. Tao, Z. Sun, Y. Xie, H. Zhang, C. Huang, Y. Zhao, Z. Liu, *J. Colloid Interface Sci.* **2011**, *353*, 269-274.

14. M. Pérez-Lorenzo, *J. Phys. Chem. Lett.* **2012**, *3*, 167-174.

15. N. Semagina, L. Kiwi-Minsker, *Catal. Lett.* **2008**, *127*, 334-338.

16. J. Boitiaux, J. Cosyns, E. Robert, *Applied Catalysis* **1987**, *32*, 145-168.

17. T. Ueno, M. Suzuki, T. Goto, T. Matsumoto, K. Nagayama, Y. Watanabe, *Angew. Chem. Int. Ed.* **2004**, *43*, 2527-2530.

18. N. Semagina, A. Renken, L. Kiwi-Minsker, *J. Phys. Chem. C* **2007**, *111*, 13933-13937.

19. O. M. Wilson, M. R. Knecht, J. C. Garcia-Martinez, R. M. Crooks, *J. Am. Chem. Soc.* **2006**, *128*, 4510-4511.

20. H. J. Freund, *Top. Catal.* **2008**, *48*, 137-144.

21. J. Silvestrealbero, G. Rupprechter, H. Freund, *J. Catal.* **2006**, *240*, 58-65.

22. J. Silvestre-Albero, G. Rupprechter, H. J. Freund, *Chem. Commun.* **2006**, 80-82.

23. Y. Pérez, M. L. Ruiz-González, J. M. González-Calbet, P. Concepción, M. Boronat, A. Corma, *Catal. Today* **2012**, *180*, 59-67.

24. a) K. N. Campbell, L. T. Eby, *J. Am. Chem. Soc.* **1941**, *63*, 216-218; b) K. Ahmad, F. M. Strong, *J. Am. Chem. Soc.* **1948**, *70*, 1699-1700; c) R. A. Max, F.E. Deatherage, *J. Am. Oil Chem. Soc.* **1951**, *28*, 110-114; d) S. A. Fusari, K. W. Greenlee, J. B. Brown, *J. Am. Oil Chem. Soc.* **1951**, *28*, 416-420; e) D. R. Howton, R. H. Davis, *J. Org. Chem.* **1951**, *16*, 1405-1413; f) W. F. Huber, *J. Am. Chem. Soc.* **1951**, *73*, 2730-2733; g) W. Oroshnik, G. Karmas, A. D. Mebane, *J. Am. Chem. Soc.* **1952**, *74*, 295-304; h) N. A. Khan, *J. Am. Chem. Soc.* **1952**, *74*, 3018-3022; i) J. A. Knight, J. H. Diamond, *J. Org. Chem.* **1959**, *24*, 400-403.

25. a) Y. Nitta, T. Imanaka, S. Teranishi, *Bull. Chem. Soc. Jpn.* **1981**, *54*, 3579-3580; b) W. Oroshnik, G. Karmas, A. D. Mebane, *J. Am. Chem. Soc.* **1952**, *74*, 3807-3813; c) W. Oroshnik, A. D. Mebane, *J. Am. Chem. Soc.* **1954**, *76*, 5719-5736; d) C. A. Brown, V. K. Ahuja, *J. Chem. Soc., Chem. Commun.* **1973**, 553-554.

26. A. K. Ghosh, K. Krishnan, *Tetrahedron Lett.* **1998**, *39*, 947-948.

27. H. Lindlar, R. Dubuis, *Org. Synth. Colloids* **1973**, *5*, 880-882.

28. M. Crespo-Quesada, A. Yarulin, M. Jin, Y. Xia, L. Kiwi-Minsker, *J. Am. Chem. Soc.* **2011**, *133*, 12787-12794.

29. Á. Molnár, A. Sárkány, M. Varga, *J. Mol. Catal. A: Chem.* **2001**, *173*, 185-221.

Part II.

1. Dimitrios Tasis.; Nikos Tagmatarchis.; Alberto Bianco.; Maurizio Prato. *Chem. Rev*. **2006**, *106*, 1105-1136

2. Qu, L. T.; Dai, L. M. *J. Am. Chem. Soc.* **2005**, *127*, 10806.

3. Yan, Y.; Zhang, M.; Gong, K.; Su, L.; Guo, Z.; Mao, L. *Chem. Mater*. **2005**, *17*, 3457.

4. (a) Banerjee, S.; Hemraj-Benny, T.; Wong, S. S. *Adv. Mater*. **2005**, *17*, 17; (b) Yan, Y.; Zhang, M.; Gong, K.; Su, L.; Guo, Z.; Mao, L. *Chem. Mater*. **2005**, *17*, 3457.

5. Banerjee, S.; Hemraj-Benny, T.; Wong, S. S. *Adv. Mater*. 2005, *17*, 17.

6. Dyke, C. A.; Tour, J. M. J. *Phys. Chem. A*,, **2004**, *108*, 11151.

7. Holzinger, M.; Abraham, J.; Whelan, P.; Graupner, R.; Ley, L.; Hennrich, F.; Kappes, M.; Hirsch, A. *J. Am. Chem. Soc*. **2003**, *125*, 8566.

8. Holzinger, M..; Steinmetz, J.; Samaille, D.; Glerup, M.; Paillet, M.; Bernier, P.; Ley, L.; Graupner, R. *Carbon* **2004**, *42*, 941.

9. Holzinger, M.; Vostrowsky, O.; Hirsch, A.; Hennrich, F.; Kappes, M.;Weiss, R.; Jellen, F.*Angew. Chem. Int. Ed*. **2001**, *40*, 4002.

10. Masayasu Taki.; Mika Desaki.; Akio Ojida.; Shohei Iyoshi.; Tasuku Hirayama.; Itaru Hamachi.;Yukio Yamamoto. *J. Am. Chem. Soc.* **2008**, *130*, 12564–12565

11. Cyrille Grandjean.; Alain Boutonnier.; Catherine Guerreiro.; Jean-Michel Fournier.; Laurence A. Mulard .; *J. Org. Chem.* **2005**, *70*, 7123-7132

12. Tao Zhang.; Min Xu.; Ling He.; Kai Xi.; Min Gu.; Zhengsheng Jiang.; *Carbon*. **2008**, *46*, 1782-1791

국문초록

I. 팔라듐 나노입자의 모양에 따른 촉매 활성에 관한 연구

알카인에서 알켄으로 선택적인 수소화 반응을 위한 촉매에 관해 많이 연구되어왔지만 주로 반응에 적용할 수 있는 물질의 범위가 좁고 반응성을 감소시키는 방법이었다. 그러나 우리는 쉽게 합성할 수 있는 큐브모양의 팔라듐을 이용하여 수소화 반응을 진행하였을 때 모양의 [100] 면에 의해 삼중결합에서 이중결합으로 빠르게, 이중결합에서 단일결합으로 느리게 환원반응이 진행되는 것을 확인할 수 있었다. 이러한 결과는 [100], [110], [111] 면으로 구성된 팔라듐 차콜을 촉매로 이용하였을 때보다 더 나은 이중결합 선택성을 나타내는 것 또한 확인하였다. 따라서 팔라듐 나노입자 모양에 따라 촉매로써 다른 반응성을 나타내는 것을 알 수 있었다.

II. 탄소 나노 튜브의 작용기 도입과 응용에 관한 연구

탄소나노 튜브는 열적, 물리적, 화학적 안정성과 높은 전기전도도와 같은 특징 때문에 다양한 분야에 사용될 수 있다. 특히 촉매의 지지체로서 이용하기 위한 다양한 연구가 진행되어왔다. 우리는 탄소나노튜브에 다양한 작용기를 도입하기 위해 나이트린 화학을 이용하였다. 또한 도입한 카르복실산 작용기에 아마이드 본드를 형성함으로 산소나 질소와 같이 비공유전자쌍을 제공할 수 있는 원자를 도입하였다. 이러한 작용기 도입은 적외선 분광법등을 통해 확인하였다. 또한 금속의 환원력에 따라 다른 환원제를 이용하여 팔라듐에는 하이드라진을, 백금에는 수소가스를 통해 환원하여 탄소나노튜브 유도체에 금속을 고정화 하였다.

완성된 백금-탄소나노튜브를 이용하여 나이트로 환원반응을 진행한 결과 높은 반응성뿐만 아니라 재사용이 가능한 촉매계를 확인할 수 있었다.